Eur. Phys. J. B **50**, 559–564 (2006)
DOI: 10.1140/epjb/e2006-00182-1

THE EUROPEAN PHYSICAL JOURNAL B

Optical absorption of a quantum well with an adjustable asymmetry

H. Yildirim[1,a] and M. Tomak[1]

Department of Physics, Middle East Technical University, Ankara 06531, Turkey

Received 25 January 2006
Published online 17 May 2006 –

Abstract. The effects of asymmetry and the electric field on the electronic subbands and the nonlinear intersubband optical absorption of GaAs quantum wells represented by a Pöschl-Teller confining potential are studied. The potential itself can be made asymmetric through a correct choice of its parameter set and this adjustable asymmetry is important for optimizing the absorption. In that way optimal cases can be created. We calculate the modified wave functions and electronic subbands variationally. The linear and the nonlinear optical intersubband absorption coefficients are calculated. Numerical results for a typical GaAs quantum well are presented. The nonlinear part of the absorption coefficient is strongly modified by the asymmetry parameters while the electric field affects it at smaller values of the parameters.

PACS. 42.65.Ky Frequency conversion; harmonic generation, including higher-order harmonic generation - 78.67.De Quantum wells

1 Introduction

The intersubband optical transitions within the conduction band of a GaAs quantum well has been observed experimentally [1]. A very large dipole strength and a narrow band width were observed. This suggests there is a strong nonlinearities associated with the intersubband transitions. Moreover, application of an electric field parallel to the growth direction to GaAs quantum well resulted in a Stark shift of intersuband transitions [2]. There are numerous studies focused on the intersubband transitions and optical absorptions [3–17] and nonlinear optical properties induced by interband and intersubband transitions [18,19] in semiconductor quantum wells. The intersubband transitions within the conduction band of semiconductor heterostructures have many device applications in the infrared region [20].

The nonlinear optical properties generally depend on the asymmetry of the confining potential. The asymmetry of the single quantum wells is obtained through changing the composition gradient of the host material or applying an electric field in the growth direction. In the calculations cited, the nonlinear optical properties are calculated by choosing an asymmetrical potential of fixed shape. However, the dependence of these properties on the well parameters may be betters studied by using a potential whose asymmetry can be adjusted and the corresponding Hamiltonian can be analytically solved.

The Pöschl-Teller potential [21] has attracted some interest in recent years [22–25]. The Pöschl-Teller potential has tunable asymmetry and the corresponding Schrödinger equation is analytically solvable in the absence of an applied electric field [21]. Its width and depth can be adjusted or it can easily become asymmetric by a correct choice of its parameter set. The tunable asymmetry of the potential, therefore, is expected to yield promising nonlinear optical properties. Tong [22] suggests several applications in semiconductor heterojunction devices and in optical systems. Tong and Kiriushcheva [23] showed that it can be used in reduction of noise in resonance tunnelling devices and other devices. Radovanovic et al. [24] worked on several intersubband absorption properties of the potential. Yildirim and Tomak [25] studied several intersubband nonlinear optical properties of the potential. We studied the effect of the these parameters on the linear and nonlinear intersubband optical absorption without an electric field [25]. The peak position and the peak value of the total absorption are strong functions of the parameters. However, there is no work on the effect of the electric field on the electronic subband structure and the optical absorption of such a potential.

In this work, we calculate the new energy levels and the modified wave functions for the ground and first excited states when an electric field is applied in the growth direction. This brings an additional asymmetry to the potential. It will be interesting to investigate its effects on the nonlinear intersubband optical absorption. The variational method with Gram-Schmidt orthogonalization

[a] e-mail: hasany@newton.physics.metu.edu.tr

procedure [26] is used as there is no analytic solutions valid for all values of the electric field to the best of our knowledge. We find that energy levels increase and the wave functions are pushed to the one side of the well with the increasing electric field. The results are in good agreement with those obtained from the calculations based on the time-independent perturbation theory. The linear and nonlinear intersubband optical absorptions are calculated. The peak values of the nonlinear term are decreased in magnitude which enhances the total absorption coefficient at larger values of the parameters. The electric field modifies the peak values of the total absorption at smaller values of the parameters rather than at their large values. The shift of the resonance energy with the increasing electric field depends on the relative magnitudes of the parameters.

The organization of this paper is as follows: in Section 2, the Gram-Schmidt orthogonalization procedure is introduced and the form of the ground state and first-excited state wave functions are presented. The expressions for the linear and the nonlinear absorption coefficient are derived within the density matrix formalism. In Section 3, numerical implementation on typical GaAs material is presented. A brief conclusion is given in Section 4.

2 Theory

Consider an electron with a charge $-|e|$ and a constant effective mass m^* in a quantum well represented by a potential $V(z)$ in the presence of an electric field F along the growth direction, z, of the well. Then the Hamiltonian of the problem is

$$H = -\frac{\hbar^2}{2m^*}\left[\frac{\partial^2}{\partial x^2}+\frac{\partial^2}{\partial y^2}+\frac{\partial^2}{\partial z^2}\right]+V(z)+qFz, \quad (1)$$

where

$$V(z) = \frac{\hbar^2\gamma^2}{2m^*}\left[\frac{\kappa(\kappa-1)}{\sin^2(\gamma z)}+\frac{\eta(\eta-1)}{\cos^2(\gamma z)}\right],\ \kappa,\ \eta>1. \quad (2)$$

The Pöschl-Teller potential , *V(z)* is governed by three parameters: κ, η, and γ. This potential has singularities at $z = 0$ and at $z = \frac{\pi}{2\gamma}$ [21]. γ is known as the width parameter, and κ, η as the depth parameters. κ and η also tune the degree of the asymmetry. The minimum of the potential occurs at smaller z values for $\kappa < \eta$ while it occurs at larger z values for $\kappa > \eta$. The potential profile is perfectly symmetric for $\kappa = \eta$. Pöschl-Teller potential resembles the profile of a diffused quantum well [27].

In the absence of the electric field, the eigenfunctions $\psi_{n,k}(\boldsymbol{r})$ and eigenenergies $\varepsilon_{n,k}$, are given respectively by

$$\psi_{n,k}(\boldsymbol{r}) = \varphi_n(z)\exp(i\mathbf{k}_\parallel\cdot\mathbf{r}_\parallel), \quad (3)$$

$$\varepsilon_{n,k} = E_n + \frac{\hbar^2}{2m^*}\left|\mathbf{k}_\parallel\right|^2, \quad (4)$$

where $\mathbf{k}_\parallel$and $\mathbf{r}_\parallel$ are the wave and position vectors in the xy plane. $\varphi_n(z)$ and E_n are the envelope wave function and transverse energy of the n^{th} subband, respectively and are the solutions of the Schrödinger equation

$$H_z\varphi_n(z) = E_n\varphi_n(z), \quad (5)$$

where H_z is the z component of the Hamiltonian H. $\varphi_n(z)$ and E_n are given by [21]

$$\varphi_n(z) = C_n\sin^\kappa(\gamma z)\cos^\eta(\gamma z) \times {}_2F_1\left(-n,\kappa+\eta+n,\kappa+\frac{1}{2};\sin^2(\gamma z)\right), \quad (6)$$

$$E_n = \frac{\hbar^2\gamma^2}{2m^*}(\kappa+\eta+2n)^2\ n = 0,1,2,\ldots \quad (7)$$

Here, C_n is the normalization constant and ${}_2F_1(a,b,c;f(z))$ is the Hypergeometric function.

The simple form of the trial wave function, $f_n(z)\exp(-\beta_n z)$, is proved to give accurate results for $n = 1$ for an infinite well [26], where $f_n(z)$ is the zero-field nth quantum well bound state and β_n is a variational parameter. However, it provides significantly different results from the numerical calculations for the higher energy levels as these trial wave functions are not orthogonal to each other [26]. We find analytic forms of orthogonalized trial wave functions by the Gram-Schmidt orthogonalization procedure [26]. This procedure requires the construction of an orthonormal set $\{\phi_0,\phi_1,\ldots\}$ from a finite or an infinite independent set $\{u_0,u_1,\ldots\}$ which is not necessarily orthonormal [26].

We suggest the following nth vector, u_n,

$$u_n(z) = \sin^\kappa(\gamma z)\cos^\eta(\gamma z) \times {}_2F_1\left(-n,\kappa+\eta+n,\kappa+\frac{1}{2};\sin^2(\gamma z)\right) \times \exp\left[-\beta_n\left(\frac{z}{L}+\frac{1}{2}\right)\right], \quad (8)$$

which is not an orthogonal set, where β_n is the nth variational parameter. The variational wave function for the ground state is

$$\phi_0 = u_0\langle u_0|u_0\rangle^{-1/2}. \quad (9)$$

The ground state energy is found by minimization of $E_0(\beta_0)$ with respect to β_0. The corresponding equation is given as

$$E_0(\beta_0) = \langle u_0|H_z|u_0\rangle\langle u_0|u_0\rangle^{-1}. \quad (10)$$

We start with

$$\theta = u_1 - \langle u_1|\phi_0\rangle\phi_0. \quad (11)$$

to find the first excited wave function and its energy. Here $\langle u_1|\phi_0\rangle$ is the inner product between the related functions. Minimization of

$$E_1(\beta_1) = \langle\theta|H_z|\theta\rangle\langle\theta|\theta\rangle^{-1} \quad (12)$$

with respect to β_1 provides us with the first excited state energy level. The corresponding wave function can be found as

$$\phi_1 = \theta\langle\theta|\theta\rangle^{-1/2}. \quad (13)$$

We consider an optical radiation of angular frequency ω applied to the system with the polarization along the growth direction, z. The incident field can be written as [28]

$$E(t) = \sum_j E(\omega_j) e^{-i\omega_j t}, \tag{14}$$

where the summation goes over all frequencies. The one-electron density matrix equation with intraband relaxation is

$$\frac{\partial \rho_{ij}}{\partial t} = \frac{1}{i\hbar}\left[H_0 - qzE(t), \rho\right]_{ij} - \Gamma_{ij}\left(\rho - \rho^{(0)}\right)_{ij}, \tag{15}$$

where H_0 is unperturbed Hamiltonian. The Γ_{ij} elements are taken to be equal to one value Γ_0 only. Equation (15) is solved via the iterative method [4,28], by noting that,

$$\rho(t) = \sum_n \rho^{(n)}(t), \tag{16}$$

with

$$\frac{\partial \rho_{ij}^{(n+1)}}{\partial t} = \frac{1}{i\hbar}\left[H_0, \rho^{(n+1)}\right]_{ij} - \Gamma_0 \rho_{ij}^{(n+1)} - \frac{1}{i\hbar}\left[qz, \rho^{(n)}\right]_{ij} E(t). \tag{17}$$

The electronic polarization $P(t)$ and the susceptibility $\chi(t)$ caused by the optical field $E(t)$ can be expressed through the dipole operator μ and the density matrix as [4,28]

$$P(t) = \frac{1}{V}\mathrm{Tr}(\rho\mu), \tag{18}$$

where V is the volume of the system and Tr stands for the trace.

The absorption coefficient and the susceptibility are related by [4]

$$\alpha(\omega) = \frac{4\pi\omega}{n_r c}\mathrm{Im}\left(\chi(\omega)\right), \tag{19}$$

where n_r is the refractive index of the system and the c is the speed of the light. By using the density matrix formalism and the iterative procedure [4,28], the linear and the third-order absorption coefficients, $\alpha^{(1)}(\omega)$ and $\alpha^{(3)}(\omega, I)$, respectively are derived. We neglect the higher-harmonic terms and consider only the steady-state response. The first- and third-order absorption coefficients are found to be

$$\alpha^{(1)}(\omega) = \frac{4\pi\omega}{n_r c}\frac{\sigma_s |\mu_{10}|^2 \hbar\Gamma_0}{\left(E_{10} - \hbar\omega\right)^2 + \left(\hbar\Gamma_0\right)^2}, \tag{20}$$

$$\alpha^{(3)}(\omega, I) = -2\omega\left(\frac{4\pi}{n_r c}\right)^2 \frac{I\sigma_s |\mu_{10}|^4 \hbar\Gamma_0}{\left(\left(E_{10} - \hbar\omega\right)^2 + \left(\hbar\Gamma_0\right)^2\right)^2} \times\left(1 - \left|\frac{\mu_{11} - \mu_{00}}{2\mu_{10}}\right|^2 \times\frac{\left\{(E_{10} - \hbar\omega)^2 - (\hbar\Gamma_0)^2 + 2E_{10}(E_{10} - \hbar\omega)\right\}}{E_{10}^2 + (\hbar\Gamma_0)^2}\right), \tag{21}$$

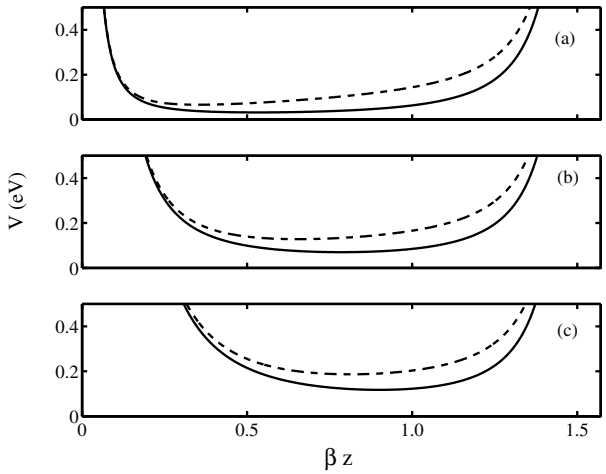

Fig. 1. The Pöschl-Teller potential profiles with (dashed-line) and without (solid line) an applied-electric field for three different κ values: 1.2, 2.0, and 2.8 in panels (a), (b), and (c), respectively. The electric field strength is $100\,\mathrm{kV\,cm^{-1}}$ and $\eta = 2$ for each curve.

respectively. Here I is the intensity of the incident field, σ_s is the density of the electrons, $E_{10} = E_1 - E_0$, and μ_{ij} is the matrix element of the dipole operator $\mu_{ij} = \langle\phi_i|qz|\phi_j\rangle$ $(i, j = 0, 1)$. The second term in equation (21) is zero when the potential is symmetric. We write the total absorption coefficient $\alpha(\omega, I)$ as

$$\alpha(\omega, I) = \alpha^{(1)}(\omega) + \alpha^{(3)}(\omega, I). \tag{22}$$

3 Numerical results and discussion

We work out the wave functions and the energy levels and then calculate $\alpha^{(1)}(\omega)$ and $\alpha^{(3)}(\omega, I)$ using numerical values for a typical GaAs quantum well in this section. These input parameters [4] are: $\sigma_s = 3 \times 10^{16}\,\mathrm{cm^{-3}}$, $\Gamma_0 = 1/0.14\,\mathrm{ps^{-1}}$, $n_r = 3.2$, $m^* = 0.067 m_0$. The length of the quantum well, L, and γ are taken to be 126.5 Å and $\frac{\pi}{2L}$, respectively.

In Figure 1, the potential profile is shown for three different κ values, namely $\kappa = 1.2$, $\kappa = 2$, and $\kappa = 2.8$ in the absence and the presence of an electric field of $100\,\mathrm{kV\,cm^{-1}}$, respectively. As would be expected, the electric field introduce an additional asymmetry and the potential becomes narrower. In all cases, the applied field increases the minimum of the potential which is expected to give higher energy levels compared to zero-field case.

The normalized wave functions of the ground and first excited levels are plotted in Figures 2 and 3, respectively. The wave functions are shifted to the direction opposite to the applied electric field. The wave functions corresponding to the potential determined by $\kappa = 1.2$ are shifted more because, the potential for the region $z < L/2$ is more confining.

The variationally calculated ground and first excited energy levels are displayed in Table 1. As the applied electric field is increased the energy levels increase also since

Table 1. The variational and perturbational calculated energy eigenvalues for the ground and first excited states in meV under the applied electric field for $\eta = 2$. The values in parenthesis are calculated by the time-independent perturbation theory. The applied electric field is 0, 25, 50, 100 kV/cm from top to bottom, respectively

$\kappa = 1.2$		$\kappa = 2.0$		$\kappa = 2.8$	
E_0	E_1	E_0	E_1	E_0	E_1
89.70 (89.70)	236.87 (236.87)	140.16 (140.16)	315.36 (315.36)	201.83 (201.83)	405.06 (405.06)
103.19 (103.20)	251.69 (251.69)	155.84 (155.85)	331.15 (331.16)	219.05 (219.06)	421.72 (421.73)
116.38 (116.38)	266.54 (266.55)	171.30 (171.31)	346.95 (346.96)	236.09 (236.11)	438.37 (438.39)
142.12 (142.01)	296.58 (296.64)	201.82 (201.83)	378.83 (378.86)	269.99 (270.04)	471.94 (471.97)

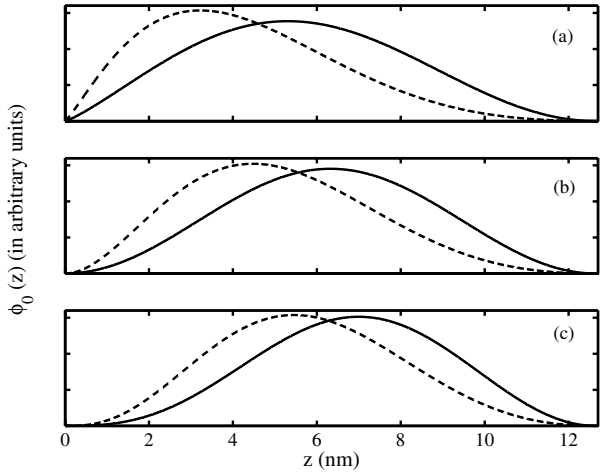

Fig. 2. The normalized ground state wave functions of the Pöschl-Teller quantum well with (dashed-line) and without (solid line) an applied electric field for three different κ values: 1.2, 2.0, and 2.8 in panels (a), (b), and (c), respectively. The electric field strength is $500\,\mathrm{kV\,cm^{-1}}$ and $\eta = 2$ for each curve.

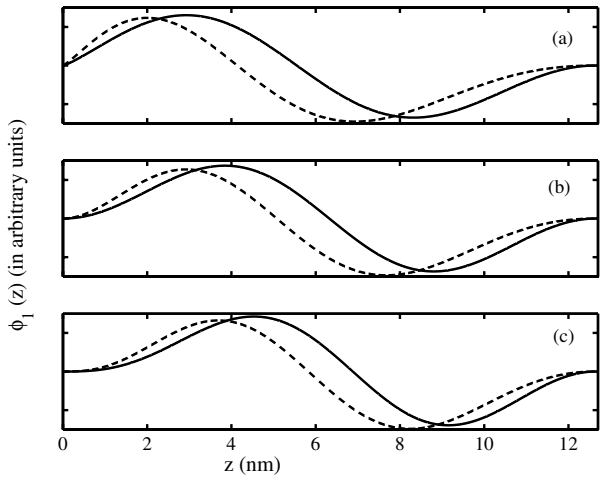

Fig. 3. The normalized first-excited state wave functions of the Pöschl-Teller quantum well with (dashed- line) and without (solid line) an applied electric field for three different κ values: 1.2, 2.0, and 2.8 in panels (a), (b), and (c), respectively. The electric field strength is $500\,\mathrm{kV\,cm^{-1}}$ and $\eta = 2$ for each curve.

the potential curve becomes narrower and its minimum is shifted upward in energy. The energy levels are not equally spaced for a fixed κ, instead they are almost linearly proportional to the applied electric field. We can explain this by the time-independent perturbation theory. For weak fields, such that [29]

$$qFL \ll \mid E_0^{(0)} - E_1^{(0)} \mid, \tag{23}$$

the shift in the nth energy level can be written as

$$\Delta_n = F\mu_{nn} + F^2 \sum_{j \neq n} \frac{\mid \mu_{nj} \mid^2}{E_n^{(0)} - E_j^{(0)}} + \ldots, \tag{24}$$

where zero in superscripts refers to the zero-field energy levels. As the first term in equation (24) dominates, it is expected that the energetic difference increases almost linearly with the applied electric field provided that κ is constant. The energy values for both states obtained from the perturbation calculations are also shown in Table 1. We see that both methods are in good agreement with each other.

In intersubband transitions most of the oscillator strength is in the $1 \longrightarrow 2$ transition (it is nearly 0.96 for an infinite well potential). Then the Thomas-Reich-Kuhn yields [30]

$$\frac{2m^*}{\hbar^2} E_{10} |z_{10}|^2 \cong 1. \tag{25}$$

That is, the enhancement of the linear absorption originates from the contribution of the optical transitions between the conduction band and the other bands of the quantum well [30]. We have seen that our calculations on the Pöschl-Teller quantum well obey equation (25) for $1 < \kappa, \eta \leq 3.0$ up to $F = 100\,\mathrm{kV\,cm^{-1}}$ and we have obtained almost constant peak values for equation (20) (not shown) if it is assumed that the electric field does not change the electron distribution in the subbands (when this assumption is not applied it is possible to enhance the peak value of $\alpha^{(1)}(\omega)$ by the electric field [4]).

When equation (22) is evaluated at the resonance frequency (i.e. $\hbar\omega \approx E_{10}$) its peak value reads

$$\alpha_p(\omega, I) = \alpha_p^{(1)}(\omega) \left[(1 - \frac{8\pi}{n_r c} \frac{Iq^2}{(\hbar\Gamma_0)^2} |z_{10}|^2 \right], \tag{26}$$

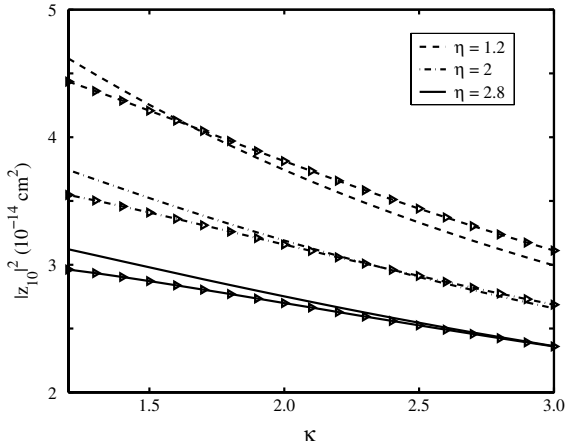

Fig. 4. $|z_{10}|^2$ as a function of κ for $\eta = 1.2$, 2.0, and 2.8 displayed by dashed-, dotted- and solid lines, respectively. The same lines labeled by triangles are drawn also in the presence of an electric field of 100 kV cm^{-1}.

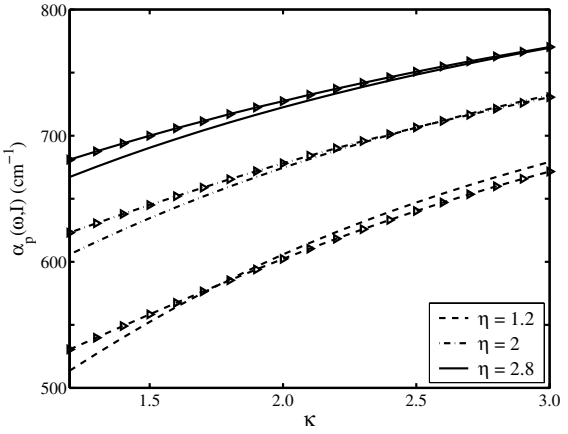

Fig. 5. $\alpha_p(\omega, I)$ as a function of κ for $\eta = 1.2$, 2.0, and 2.8 displayed by dashed-, dotted- and solid lines, respectively. The same lines labeled by triangles are drawn also in the presence of an electric field of 100 kV cm^{-1}.

where p in subscripts implies peak value of the quantity. Our detailed calculations on the second term in equation (21) (not shown) say that the contribution due to this term to $\alpha^{(3)}(\omega)$ is very small. Hence we can safely ignore it in calculations. Then the problem reduces to maximize $|z_{10}|^2$. We plot $|z_{10}|^2$ as a function of κ in Figure 4. In the figure, the results obtained when an electric field of 100 kV cm^{-1} is applied are presented with lines having triangles. It is obvious that $|z_{10}|^2$ is inversely proportional to κ and η. This is expected since the larger parameters we put the narrower wells we obtain and in an infinite quantum well $|z_{10}|^2 \propto L^2$. The electric field does not alter $|z_{10}|^2$ significantly. But if relatively larger electric field strengths are considered it is possible [4] to get larger values of $|z_{10}|^2$. Regarding equation (26) we conclude that larger values of κ, and η will give larger $\alpha_p(\omega, I)$. This is verified in Figure 5 in which the $\alpha_p(\omega, I)$ is plotted as a function of κ. As it is said above the electric field does not induce any significant enhancement.

The intersubband transition energy E_{10} is plotted as function of κ in Figure 6. It is clearly seen that the transition energy increases with increasing κ and η. The interesting point is that the application of the electric field yields blue-shift in the transition energy as η becomes larger while it induces red-shift in the transition energy as κ becomes larger.

The linear $\alpha^{(1)}(\omega)$, the nonlinear absorption coefficient $\alpha^{(3)}(\omega, I)$, and the total absorption coefficient $\alpha(\omega, I)$ as functions of the incident photon energy at $I = 1.0\,\mathrm{MW/cm^2}$ for an applied electric field of 100 kV cm^{-1} are shown in Figure 7 to illustrate the conclusions above. As expected, $\alpha^{(1)}(\omega)$ is almost constant regardless of the changes in the parameters while $\alpha(\omega, I)$ is higher for larger values of the parameters. The electric field does not make any enhancement in $\alpha^{(1)}(\omega)$ while it does little in $\alpha(\omega, I)$. The resonance energies which occur at $\hbar\omega = E_{21}$ are blue-shifted for smaller κ while they are red-shifted for larger κ as mentioned above.

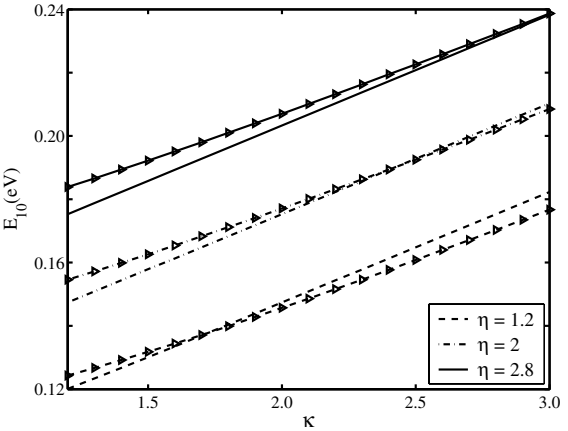

Fig. 6. E_{21} as a function of κ for $\eta = 1.2$, 2.0, and 2.8 displayed by dashed-, dotted- and solid lines, respectively. The same lines labeled by triangles are drawn also in the presence of an electric field of 100 kV cm^{-1}.

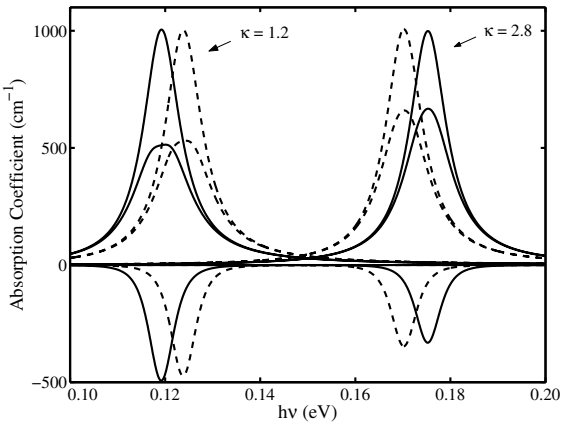

Fig. 7. The linear, the nonlinear, and the total absorption coefficient with (dashed-lines) and without (solid lines) an applied electric field for two different κ values: 1.2 and 2.8. The applied electric field is 100 kV cm^{-1} and η value is taken as 1.2.

4 Conclusion

In this work, we study the effects of the electric field on the conduction subband structure and the intersubband optical absorption of the Pöschl-Teller QW. The new energy levels and wave functions have are variationally calculated using Gram-Schmidt orthogonalization procedure. The energy levels increase in the same direction with the increasing applied electric field. The wave functions are shifted to the same side of the well. Although, the ground state wave function is shifted to the $z < L/2$ region significantly, the excited state wave function still have a considerable amplitude in the $z > L/2$ region even at $F = 500\,\mathrm{kV\,cm^{-1}}$. The results of variational calculations are compared with the results we obtain from the time-independent perturbation theory. They are found to be in good agreement with each other up to an electric field of $100\,\mathrm{kV\,cm^{-1}}$. We write the total absorption coefficient as a function of $|z_{10}|^2$ which allows us to investigate its dependence on the parameters, κ and η. The total absorption coefficient is increased as the κ and η are increased together. The electric field does not affect significantly the total coefficient at larger values of the parameters, its main effect is only on the resonance energy. The peak positions are blue-shifted as η increases and κ decreases and red-shifted in the opposite case with the increasing electric field. We have used the variational method in this work, but the main conclusions will not change if one uses more precise methods of calculations. Although we have used a constant effective mass in the Hamiltonian, a more realistic case should take into account the variation of the effective mass along the growth direction. But, for wide quantum wells, such as the one used here, the difference in the ground state energy is negligibly small when m^* is considered variable [27].

References

1. L.C. West, S.J. Eglash, Appl. Phys. Lett. **46**, 1156 (1983)
2. A. Harwitt, J.S. Harris, Appl. Phys. Lett. **50**, 685 (1987)
3. D. Ahn, S.L. Chuang, Phys. Rev. B **35**, 4149 (1987)
4. D. Ahn, S.L. Chuang, IEEE J. Quantum Electron. **QE-23**, 2169 (1987)
5. P. von Allmen, Phys. Rev. B **46**, 13351 (1992)
6. S.L. Chuang, M.S.C. Luo, S. Schmitt-Rink, A. Pinczuk, Phys. Rev. B **46**, 1897 (1992)
7. C. Sirtori, F. Capasso, D.L. Sivco, A.Y. Cho, Phys. Rev. Lett. **68**, 1010 (1992)
8. A.G. Petrov, A. Shik, Phys. Rev. B **48**, 11883 (1993)
9. I.K. Marmorkos, S.D. Sarma, Phys. Rev. B **48**, 1544 (1993)
10. C. Sirtori, F. Capasso, J. Faist, S. Scandolo, Phys. Rev. B **50**, 8663 (1994)
11. R.J. Warburton, C. Gauer, A. Wixforth, J.P. Kotthaus, B. Brat, H. Kroemer, Phys. Rev. B **53**, 7903 (1996)
12. S. Tsujino, M. Rufenacht, H. Nakajina, T. Noda, C. Metzner, H. Sakaki, Phys. Rev. B **62**, 1560 (2000)
13. I. Shtrichman, C. Metzner, E. Ehrenfreund, D. Gershoni, K.D. Maranowksi, A.C. Gossard, Phys. Rev. B **65**, 035310 (2002)
14. R.N. Riemann, C. Metzner, G.H. Dohler, Phys. Rev. B **65**, 115304 (2002)
15. A. Mizel, I. Shtrichman, D. Gershoni, Phys. Rev. B **65**, 235313 (2002)
16. J. Li, C.Z. Ning, Phys. Rev. B **70**, 125309 (2004)
17. A.A. Batista, D.S. Citrin, Phys. Rev. Lett. **92**, 127404 (2004)
18. G. Almogy, A. Yariv, J. Nonlin. Opt. Phys. **4**, 401 (1995)
19. J.B. Khurgin, Semicond. Semimetals **59**, 1 (1999)
20. H.C. Liu, F. Capasso, *Intersubband transitions in quantum wells: Physics and device applications I* (Academic Press, San Diego CA, 2000)
21. S. Flugge, *Practical Quantum Mechanics I* (Springer-Verlag, Berlin Heidelberg, 1971)
22. B.Y. Tong, Solid State Communications **104**, 679 (1997)
23. B.Y. Tong, N. Kiriushcheva, Phys. Lett. A **229**, 49 (1997)
24. J. Radovanović, V. Milanavić, Z. Ikonić, D. Indjin, Phys. Lett. A **269**, 179 (2000)
25. H. Yıldırım, M. Tomak, Phys. Rev. B **72**, 115340 (2005)
26. D. Ahn, S.L. Chuang, Phys. Rev. B **49**, 1450 (1986)
27. P. Harrison, *Quantum Wells, Wires and Dots* (Jonh Wiley and Sons, New York, 2000)
28. R.W. Boyd, *Nonlinear Optics* (Academic Press, San Diego, 2003)
29. J.J. Sakurai, S.F. Tuan, *Modern Quantum Mechanics* (Addison-Wesley, USA Heidelberg, 1994)
30. E. Rosencher, Ph. Bois, Phys. Rev. B **14**, 11315 (1991)